28 March 1980, Volume 207, Number 4438 **SCIENCE**

East Pacific Rise: Hot Springs and Geophysical Experiments

RISE Project Group:

F. N. Spiess, Ken C. Macdonald, T. Atwater, R. Ballard
A. Carranza, D. Cordoba, C. Cox, V. M. Diaz Garcia
J. Francheteau, J. Guerrero, J. Hawkins, R. Haymon
R. Hessler, T. Juteau, M. Kastner, R. Larson, B. Luyendyk
J. D. Macdougall, S. Miller, W. Normark, J. Orcutt, C. Rangin

Summary. Hydrothermal vents jetting out water at 380° ± 30°C have been discovered on the axis of the East Pacific Rise. The hottest waters issue from mineralized chimneys and are blackened by sulfide precipitates. These hydrothermal springs are the sites of actively forming massive sulfide mineral deposits. Cooler springs are clear to milky and support exotic benthic communities of giant tube worms, clams, and crabs similar to those found at the Galápagos spreading center. Four prototype geophysical experiments were successfully conducted in and near the vent area: seismic refraction measurements with both source (thumper) and receivers on the sea floor, on-bottom gravity measurements, in situ magnetic gradiometer measurements from the submersible *Alvin* over a sea-floor magnetic reversal boundary, and an active electrical sounding experiment. These high-resolution determinations of crustal properties along the spreading center were made to gain knowledge of the source of new oceanic crust and marine magnetic anomalies, the nature of the axial magma chamber, and the depth of hydrothermal circulation.

In April 1976 a group of ocean-oriented earth scientists gathered in La Jolla to discuss ways in which newly available capabilities for detailed studies of the sea floor, particularly manned small submersibles, might best be further developed and used in the Pacific Ocean (*1*). Although most of those at the meeting were from U.S. institutions, there were also representatives from France, which has operational deep submersibles, and Mexico, which has a number of potentially interesting offshore areas. An outcome of this meeting was the inception of the Rivera Submersible Experiments (RISE) program, whose results are the subject of this article.

The plate tectonic model of the earth's crust has focused the attention of marine geologists on the oceanic edges of the plates—the rise crests, transform faults, and trenches—as the regions in which investigations would be most likely to lead to an improved understanding of fundamental geological processes. The existence of exposed, small-scale phenomena at depths easily reached by today's submersibles led us to concentrate on the rise crests as particularly informative sites. Here one can observe the creation of new crust, phenomena relevant to the beginning of crustal motion, metallogenesis, hydrothermal effects, and new types of benthic biological communities. These regions have been the focus of fine-scale investigations with unmanned systems for many years (*2-5*) while more recently the FAMOUS project (*6-9*) and investigations of the Galápagos spreading center (*10*) have included major submersible programs as well.

The principal technical aspect in which the RISE program differed from the FAMOUS and Galápagos spreading center projects was a thrust to develop and exploit geophysical measurement capabilities which the submersibles and unmanned vehicles at that time did not possess. The result was a plan that emphasized physical measurements with complementary geological observations and sampling. Four geophysical experiments would be conducted to provide in situ measurements of rock magnetization; measurements of elastic (sound) wave propagation over short, shallow paths in the sea floor; very accurate gravity measurements (10 to 100 times as accurate as measurements made at the sea surface); and measurements of very low-frequency (0.2 to 2 hertz) electromagnetic propagation through the sea-floor material. The possibility of directly measuring crustal strain patterns was discussed initially but deferred in a later decision.

Our long-range goal is to investigate sites representative of the full range of known spreading rates (and related different morphologies) beyond the 20 to 40 millimeters per year characteristic of the Mid-Atlantic Ridge. The work reported here was carried out on the East Pacific Rise crest at 21°N (Fig. 1), where the Pacific and Rivera plates are separating at about 60 mm/year. This leaves for the fu-

F. N. Spiess, K. C. Macdonald, C. Cox, J. Hawkins, R. Haymon, R. Hessler, M. Kastner, J. D. Macdougall, S. Miller, and J. Orcutt, Scripps Institution of Oceanography, University of California, San Diego, La Jolla 92093; T. Atwater, Department of Earth and Planetary Sciences, Massachusetts Institute of Technology, Cambridge 02139; R. Ballard, Woods Hole Oceanographic Institution, Woods Hole, Massachusetts 02543; A. Carranza and V. M. Diaz Garcia, Centro de Ciencias del Mar y Limnología, Universidad Nacional Autónoma de México, México 20, D.F.; D. Cordoba and J. Guerrero, Instituto de Geología, Universidad Nacional Autónoma de México; J. Francheteau, Centre Océanologique de Bretagne, Centre National pour l'Exploitation des Océans, Brest 29N, France; T. Juteau, Laboratoire de Minéralogie-Pétrographie, Université Louis Pasteur, 67084 Strasbourg Cedex, France; R. Larson, Lamont-Doherty Geological Observatory, Palisades, New York 10964; B. Luyendyk, Geology Department, University of California, Santa Barbara 93106; W. Normark, Office of Marine Geology, U.S. Geological Survey, Menlo Park, California 94025; and C. Rangin, Institut de Géologie, Université de Paris, Paris, France.

ture other locations in the faster range (up to 180 mm/year); they are perhaps more exciting because of their dynamics, but are far from shore, in the equatorial Pacific, and their study is barely feasible today in view of the lack of adequate tending facilities for *Alvin*.

Three previous investigations have been carried out at the 21°N site with an unmanned deep-tow system (*11*) to document fine-scale topography and magnetic field (*3, 12–15*), and as a companion to RISE there was a 1978 expedition, CYAMEX (*16–18*) with the French submersible *Cyana*.

RISE was carried out from late March to early May 1979, using the submersible *Alvin* (*19*), its catamaran-style tender *Lulu* (both operated by Woods Hole Oceanographic Institution), and the research vessels (R.V.) *Melville* and *New Horizon* operated by Scripps Institution of Oceanography. On the first leg, with *Melville*, we used the Scripps deep-tow system (*11*) and Woods Hole's versatile ANGUS camera sled (with temperature sensors). These systems were used to install the necessary transponder net, to carry out additional surveys for detailed dive site selection, and to reconnoiter for signs of hydrothermal activity and additional sulfide mounds of the type seen by the French workers (*17*) during CYAMEX. These preliminaries were all successful and sites suitable for the gravity profile, the short-range seismic experiment, and the sulfide mound studies were all located in an active hydrothermal region.

The principal diving leg was in the southwestern portion of the crestal area already mapped (Fig. 2). In 12 dives we carried out the planned short-range seismic and gravity measurements (with collateral geological observations and rock sampling). As hydrothermal activity was found, we investigated this phenomenon, observing vents with water as hot as 380° ± 30°C and their associated sulfide mounds, as well as cooler (20°C) springs with dense biological assemblages similar to those at the Galápagos spreading center (*10*). While the submersible work was in progress, the low-frequency electromagnetic work and further hot spring mapping with ANGUS were carried out from R.V. *Melville*. On the third leg we concentrated on the magnetic measurements program at the reversal area and performed additional observations and sampling in the sulfide mound–hot spring sites.

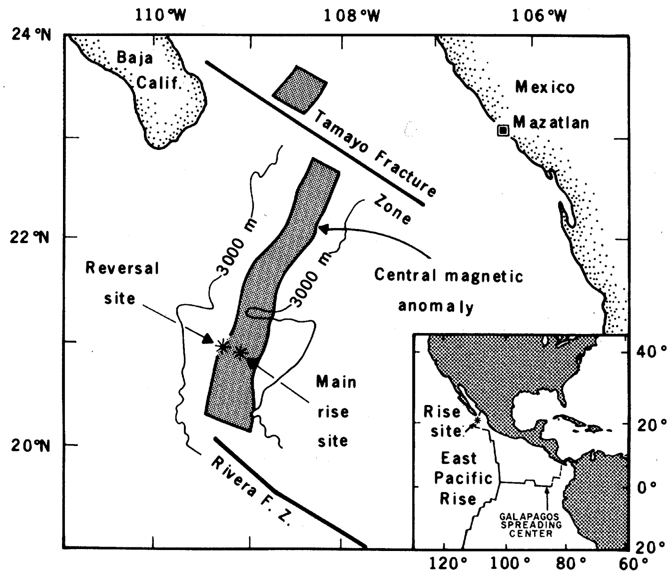

Fig. 1. Location of RISE program research sites in relation to the East Pacific Rise and Galápagos spreading center in the equatorial Pacific Ocean.

Geological Background

The crestal region discussed here, as defined by deep-tow studies (*13, 15*), is a 5-kilometer-wide axial block elevated about 80 meters above the adjacent rise flanks (Fig. 2). Based on the magnetic reversal time scale, the crust at this location formed within the last 100,000 years. The block is bounded by steep, discontinuous, elongate, constructional volcanic slopes which, taken together, show the most pronounced linearity of any features in this region. In the northeast part of the area the block is well defined on both sides, but to the southwest the relief increases to more than 100 m on the northwest side while the southeast boundary becomes indistinct.

Within the block most local relief is less than 75 m and consists of irregular volcanic peaks and ridges with some lineated fault-bounded ridges and troughs (Figs. 2 and 3). Its mean depth decreases from 2650 to 2600 m in 10 km along the strike to the southwest, with concurrent changes in local relief evidenced by the occurrence of fewer linear, steep-sided troughs.

On the basis of deep-tow work (*13, 15*) augmented by observations from *Cyana* (*16*), one can distinguish three volcanic-tectonic zones within the axial block (Fig. 3). The innermost extrusion region is flanked by a faulted and fissured extensional zone, which is in turn bounded by abyssal hills formed by back-tilted fault-block terrane. These are referred to here as zones 1, 2, and 3, respectively (*16*).

The width of zone 1, which is the area of freshest lava flows and has at most a light dusting of sediment, varies from about 600 to a little over 1000 m. It is relatively free of faults and fissures and is characterized by a discontinuous axial ridge 20 to 80 m high. In the northeast this terrane is largely formed of pillow lavas; to the southwest there are extensive lava lakes.

Although the flanking extensional zone (zone 2) is not symmetrical in width or relief on opposite sides of the rise axis, its morphology is distinctly linear. In contrast with the volcanic constructional features of the extrusion zone, this region is characterized by open fissures and horsts and grabens with relief of meters to tens of meters, mostly aligned with the regional orientation of the rise crest. Sediment-free talus slopes here attest to quite recent displacements.

In zone 3, abyssal hill or tilted fault-block terrane, active fissuring appears less common and vertical offsets on a few faults produce linear ridges several kilometers long. The transition between zones 2 and 3, best defined by direct submersible observation, commonly occurs along axially facing fault scarps with large vertical displacements that form the ridges along the edges of the axial block.

Although the relief in zone 3—tens of meters here and at the Galápagos spreading center—contrasts dramatically with the hundreds of meters encountered in the FAMOUS area, the three zones at the different sites are remarkably similar.

Observations from *Cyana* in the adjacent northern (CYAMEX) area confirmed that most of zone 1 consists of pillow lava flows, with sheet flows limited to topographic lows. In the RISE area, however, sheet flows are more extensive and in places form most of the zone, although there is a low axial pillow ridge, which is the site of most of the hydrothermal activity. CYAMEX work established that the sheet flows, especially along the axis, are associated with "fossil" lava lakes that are commonly more than 5 m in depth and hundreds of meters across, including collapse areas that show pillars and lake margins with an apparent layering of alternating glass and crystalline basalt. This pseudolayering consists of chill-zone material and is thought to record lava levels within the lakes during drainback or lateral outflow from these inflation features (*20, 21*). The lava lakes may have been fed by vents that formed the pillow ridge.

The glassy surfaces of fresh submarine basalts and fragile glassy buds and projections on fresh pillow lavas are short-lived and provide an indication of relative age, as does the thickness of accumulated sediments. The extrusion zone is free of sediment cover; glassy surfaces on pillow and sheet flows and projections

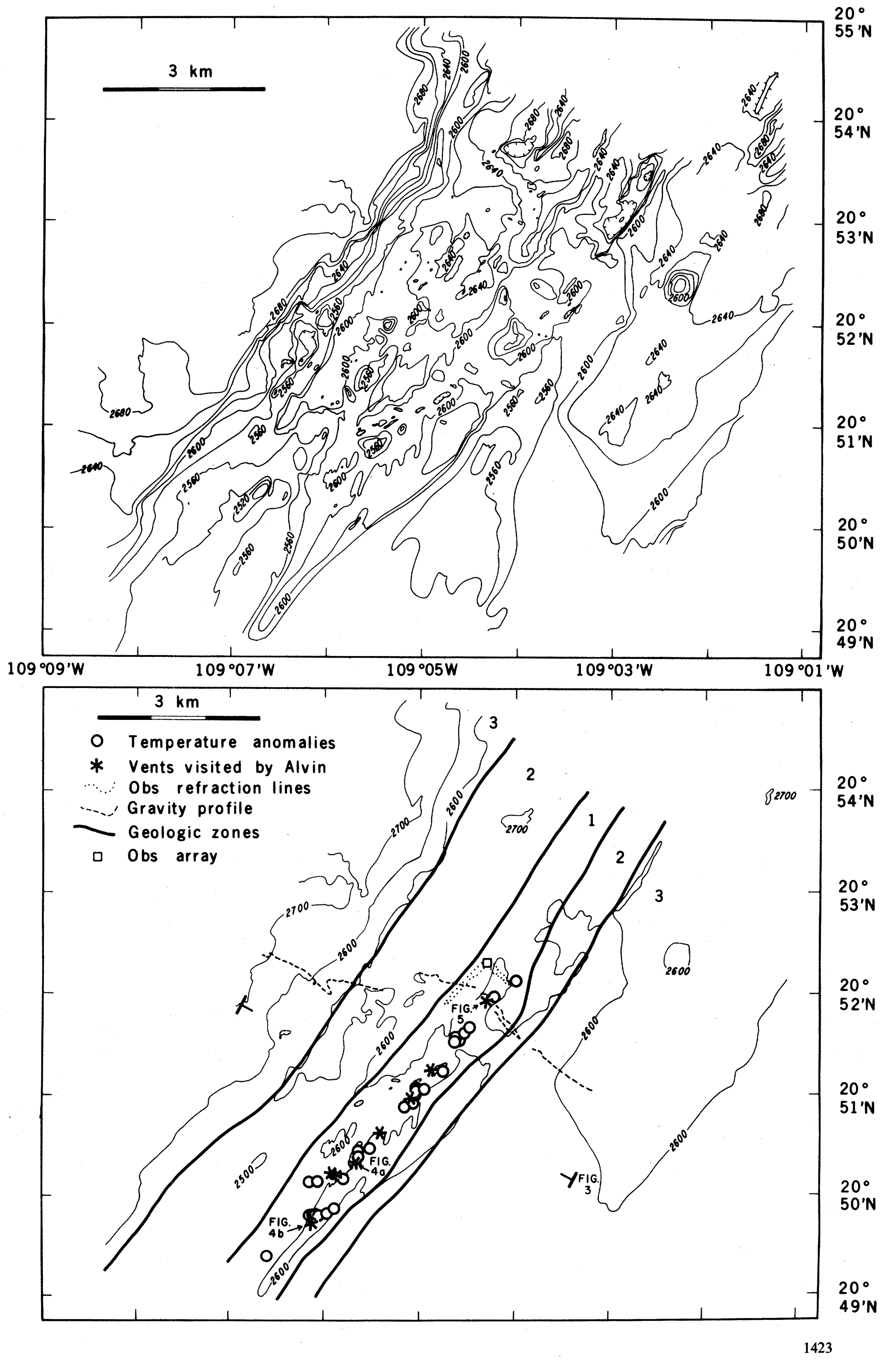

Fig. 2. Bathymetry of the RISE research area as determined with the deep-tow narrow-beam echo sounder with acoustic transponder position control. Depths are in meters, based on the sound velocity profile for the area. Lower section includes outlines of the geologic zones discussed in the text: extrusion region (zone 1), extensional zone (zone 2), and major block faulting (zone 3). Note that the vents occur in a linear zone only 200 to 300 m wide within zone 1. Eight of the 25 vents mapped were examined with *Alvin*.

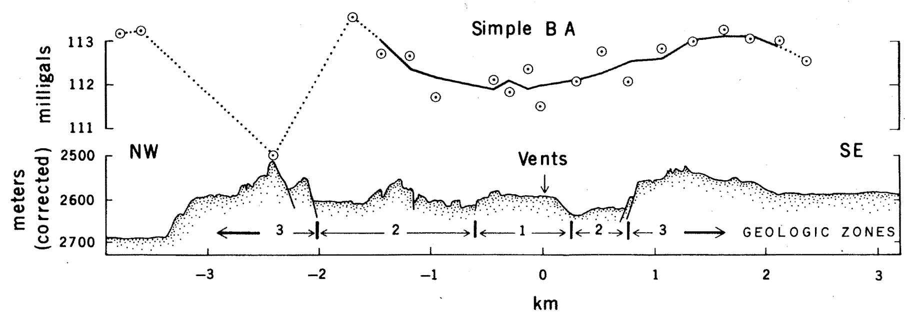

Fig. 3. Bathymetric and gravity profiles across the East Pacific Rise crest. Profile locations and zone designations are given in Fig. 2. Bathymetry is from the narrow-beam sounder of the deep-tow system. The plate boundary axis (0 km) is marked by a central volcano and active hydrothermal venting on this profile. Gravity anomaly (1 mgal $\simeq 10^{-6}g$) is derived from measurements made with *Alvin* firmly on the sea floor, corrected for gross topographic effects [Bouguer anomaly (*BA*)]. The solid line is a three-point running mean. The gravity minimum at −2.5 km is caused primarily by local topography, while that at the spreading center (zone 1) is caused by the presence of low-density material in the crust, possibly a shallow magma chamber.

on pillows are clearly observable even under light sediment dusting in the slightly older terrane within the zone. In the extension zone, glassy surfaces on the pillows are much less common, and the sediment thickness increases away from the axis. Near the outer edge of this zone, 40 to 50 percent of the pillow lava relief may be buried. Outside the extension zone, pillow lavas are nearly completely buried locally.

That the sea floor increases in age with distance from the axis is not true everywhere. Anomalously thin sediment cover and relatively fresh sheet flow basalts (which are more quickly buried than pillow flows) were observed in the extension zone and even off the axial block. The freshest flows observed on the westernmost dive, for example, were in the valley west of the axial block and not in the extension zone where the dive started. Apparently, large areas somewhat off-axis can occasionally be buried by extensive sheet flows whose source may be the same magma chamber that feeds zone 1.

Scattered evidence of past hydrothermal activity—primarily colored stain on rocks exposed at scarps—exists throughout the axial block, including one cluster of inactive sulfide mineral mounds (*17*) observed from *Cyana* on the boundary between zones 1 and 2.

Hydrothermal Vents

When this expedition began, the only major example of deep-sea hydrothermal activity was at the Galápagos spreading center, where vents were found in 1976 (*22–25*) characterized by temperature differences of 0.1°C. Subsequent submersible operations documented anomalies of 15° to 20°C and made the exciting discovery of associated dense faunal concentrations (*10, 26*). During RISE, our early measurements of temperature anomalies were quickly followed by submersible views of Galápagos-type vents (dense benthic populations and 20°C water in 2°C surroundings) and then by observations of spectacular hot-water jets with temperatures up to 380° ± 30°C precipitating metal sulfides onto the fresh basalt sea floor at the rise axis.

Twenty-five temperature anomalies indicating vents were documented with the ANGUS camera and temperature probe system, and eight of these were examined during submersible dives. The temperature spikes were confined to a band 100 to 200 m wide and about 6 km long, close to the rise axis in the southern part of the area. In spite of intense exploration with instruments towed near the bottom in the 2 by 10 km central portion of the region under study, no other sources have been located. In contrast to this very linear distribution, the vents at the Galápagos center, while still lying in the central extrusional zone, occur in groups along en echelon lines oriented about 15° to the axial direction.

The vents can be divided into two broad classes: Galápagos-type warm-water vents and sulfide mound hot-water vents, with the first type predominating in the northeast part of the band and the second type predominating at the southwest end (Figs. 2 and 4). That this along-axis zonation is probably transient is suggested by the weathered sulfide mounds found near some of our warm-water vents and found by the French (*17*) somewhat off-axis in the adjacent area to the northeast, where there no longer appears to be any concentrated hydrothermal activity. These two very different surficial manifestations of this phenomenon may be linked in evolutionary fashion, although not enough information is available yet to determine which form would be the older. The southernmost dive of *Alvin* and one lowering of ANGUS suggest that we may have defined the extent of this hydrothermal system to the southwest.

The Galápagos-type vents observed at 21°N emit warm water from hairline cracks and small fissures in the pillow ridge terrane over an area 10 to 30 m across. The venting water is generally clear and temperatures as high as 23°C were recorded close to major outlets. Mixing with the surrounding 1.8°C water is rapid. Directly above one vent of this type the temperature was about 0.3°C above ambient at an elevation of 10 m, while at a corresponding distance away laterally the anomaly was less than 0.1°C. Inactive sulfide mounds were observed on one *Alvin* dive within a few tens of meters of a warm vent.

The fauna associated with these vent areas are their most visible feature (Fig. 5). On approaching a vent field one usually sees a number of galatheid crabs and then patches of large (25-centimeter long) conspicuous white clams (vesicomyid bivalve *Calyptogena*, tentatively *C. elongata*); the clams are mostly dead in the outlying areas, but, closer in, living animals predominate. The surfaces of the lava pillows usually bear white-tubed serpulid polychaetes, so abundant in some areas that the surfaces seem fully encrusted.

Most prominent in the field, usually clustered densely around a major warm-water vent, are giant tube worms, vestimentiferan pogonophorans (Fig. 5); these are 2 to 3 cm in diameter and up to 3 m tall and have red, gill-like crowns (the only part of the living animal exposed) that may be withdrawn quickly in response to a threat, as from one of the many brachyuran crabs in the vicinity. All of these organisms have also been found at the Galápagos vents. A small, lightly colored eel-like fish, possibly an ophidiid, was seen here for the first time but is more abundant near the hot vents. Two different archaeogastropod limpets seen at Galápagos were also collected here, and photographs show a third living on the shells of live vesicomyids. Some of the animals characteristic of Galápagos (*26*) were not observed here—for example, small anemones and mussels.

The similarity of the East Pacific Rise and Galápagos Rift fauna suggests that these vent communities are widespread and that their species are equipped with sophisticated dispersal mechanisms well suited for the detection of the discontin-

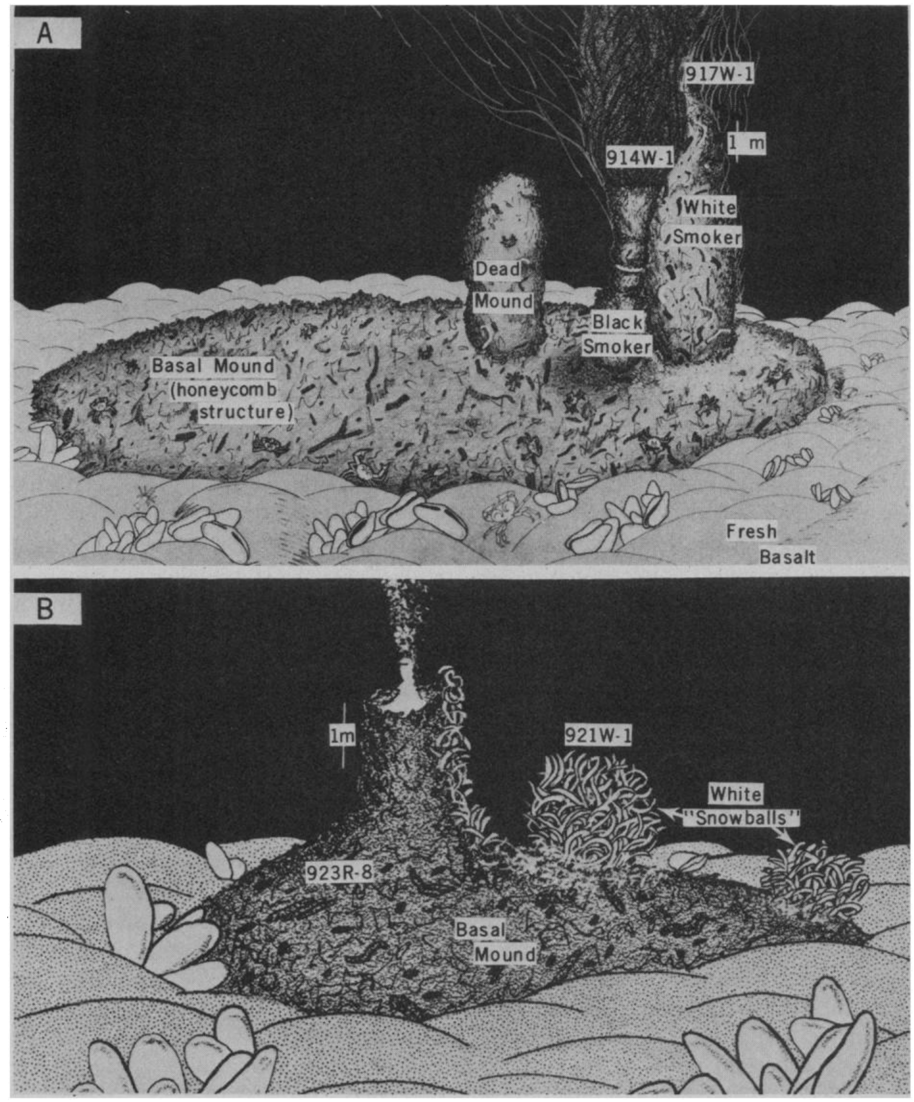

Fig. 4 (top right). Sketches of hot-water vents at locations indicated in Fig. 2, after sketches made by (A) T. Juteau and (B) C. Rangin during their observational dives. The black smoker is similar to that shown on the cover, at which 380° ± 30°C water temperatures were measured. The highest open-ocean hydrothermal temperature measured before this was 22°C at the Galápagos spreading center. Temperatures of water from "snowballs" were measured at ≃ 330°C. Specific rock and water samples discussed in the text are noted.

uous and ephemeral vent conditions. The cause of faunal differences is completely unknown, and biogeographic or ecological mechanisms are equally possible. Unfortunately, the Galápagos and East Pacific Rise are in the same ocean sector; therefore we must wait for more distant discoveries to demonstrate whether the community is worldwide.

In contrast to the biology-dominated Galápagos-type vents, the sulfide mound hot-water vents are most notable for their geological attributes. In these, the water flows out through a limited number of discrete chimneys or stacks, which are superposed on basal mounds built directly on fresh basalt pillows or flows (Fig. 4 and cover). The basal structures, similar to the CYAMEX sulfide mounds, are oxidized to Halloween colors of ocher, orange, and black and have overall lateral dimensions up to 15 by 30 m. They are honeycombed with a cross-cutting network of fossilized worm tubes. Vent constructions 1 to 5 m high rise above the base mound elevations of 2 m or more, and hydrothermal effects (staining, organisms, millimetric manganese coatings) extend tens of meters away from the vents (Fig. 4).

Edifices atop the mounds are classed as either black or white, and those venting particulates are dubbed smokers. The black chimneys are free of organisms. These "organ pipes" are as much as 30 cm in diameter and are occasionally fluted or capped by porous rock. High-temperature waters (> 350°C) spouting at high velocities (meters per second) from black chimneys are either clear or black with suspended particulates, which settle out to form a black sediment around the chimney structures (cover). The white chimneys are covered with worm tubes and thrive with worms and crabs. Structurally, they vary from chimneys to hummocky stacks to spherical "snowballs" (Fig. 4). Warm waters (32° to 330°C), clear to milky with white particulates, emanate gently from these features and deposit white sediment around the chimney bases.

The snowballs are the most striking biological feature associated with the hot

Fig. 5. Photograph of warm vent area at location shown in Fig. 2. Vents of this type emitted water at temperatures up to 23°C from fissues and hairline cracks in fresh pillow lava terrane. Clear vent water is present but not visible in this photograph. Animals in view are giant tube worms (vestimentiferan pogonophorans), clams (vesicomyid bivalve *Calyptogena*), and galatheid crabs. Limpets can be seen attached to some of the clam shells.

Table 1. Analyses of samples from hot-water vents (see Fig. 4) and deep East Pacific waters. Analyses were performed by J. Gieskes.

Sample	Cl* (per mil)	Ca* (m*M*)	Mg* (m*M*)	H_4SiO_4* (μM)	Li* (μM)	Mn† (ppm)
914W-1	19.17	13.60	52.81	234	31.2	0.320
917W-1	19.17	10.63	52.74	255	28.0	0.320
Deep East Pacific waters (2000 m)	19.17	10.53	53.40	180	27.0	< 0.04

*Analyzed by titration. †Analyzed by colorimetry.

vents. The sponge-like mass of tubes capping these vents is apparently formed by a pink terebillomorph polychaete (possibly a new family), which was observed to dart completely out into the water and then return to its tube. The slopes at the bases of the chimneys are populated with galatheids, brachyurans, and the eel-like ophidiid fish. A very primitive scalpellid barnacle of a new genus (*27*) was collected from such a site. Although the temperature of the exiting water is high (380° ± 30°C), the lateral gradients are so steep that even the chimney-top–dwelling polychaete is probably bathed in far cooler water.

The discovery of the high-temperature vents raises exciting questions for future biological research. This is apparently the first time water temperatures well in excess of the boiling point at 1 atmosphere have been found in open contact with the biosphere. Since high pressure, which permits these superheated conditions, counteracts some of the destructive effects of high temperature on biochemical systems, it is not unreasonable to wonder whether life may exist at higher temperatures here than elsewhere on the earth. A sample of 300°C water did not contain bacteria (*28*), but there is no other evidence on this point and this potentially important question must await further investigation.

Three water samples were taken from the vicinity of the vents (Fig. 4) with equipment originally designed for use from deep-tow (*11*). Since it was not possible to place the bottles exactly in the vents, there was considerable dilution; however, all samples have significantly elevated concentrations of ^{3}He and total He (*29*), implying a mantle contribution. Covariance of hydrogen and methane with helium in the vent water samples suggests that these gases are also mantle-derived (*30*). Analyses of filtered samples from adjacent black and white vent waters (Table 1) show similar enrichments (calcium, lithium, silicon, and manganese) and depletions (magnesium) relative to normal seawater. These are consistent with the trends observed in Galápagos hydrothermal fluids (*10*) and in basalt-seawater hydrothermal experiments (*31, 32*).

The black vent water precipitates consist primarily of pyrrhotite in hexagonal platelets (Fig. 6), plus pyrite, sphalerite, and Cu-Fe sulfides. Chemical composition of the pyrrhotite indicates a formation temperature of about 300°C, consistent with measured water temperatures. White vent particulates, apparently particles from worm tubes and chimney sulfides, are predominantly pyrite globules, barite rosettes, and ubiquitous amorphous silica.

In the heterogeneous mound and chimney materials the dominant solid phases, identified by x-ray diffraction, scanning electron microscopy, and electron microprobe studies, include sphalerite (ZnS), pyrite (FeS_2), and chalcopyrite ($CuFeS_2$). Other sulfides of zinc, iron, and copper are also present in minor quantities (wurtzite, pyrrhotite, marcasite, bornite, cubanite, and chalcocite). Calcium and barium sulfates (anhydrite, gypsum, and barite) and oxides of iron and silicon (goethite, and amorphous iron oxyhydroxide and silica) are quite common; native sulfur occurs often; and the magnesium silicate, talc, was found on one sample. The most significant vent minerals beyond those found in the CYAMEX inactive mounds (*17*) are pyrrhotite, anhydrite, barite, and talc. Cobalt, lead, silver, cadmium, and manganese were all detected in the CYAMEX samples at concentrations up to a few parts per thousand. The numerous and highly heterogeneous samples of the RISE collection are being analyzed for these and other elements.

The honeycomb rocks from basal mounds consist mainly of sphalerite and pyrite, lesser amounts of chalcopyrite, minor wurtzite and marcasite, amorphous silica and iron oxyhydroxides, and traces of native sulfur. Brittle, platy white precipitates coating the tube

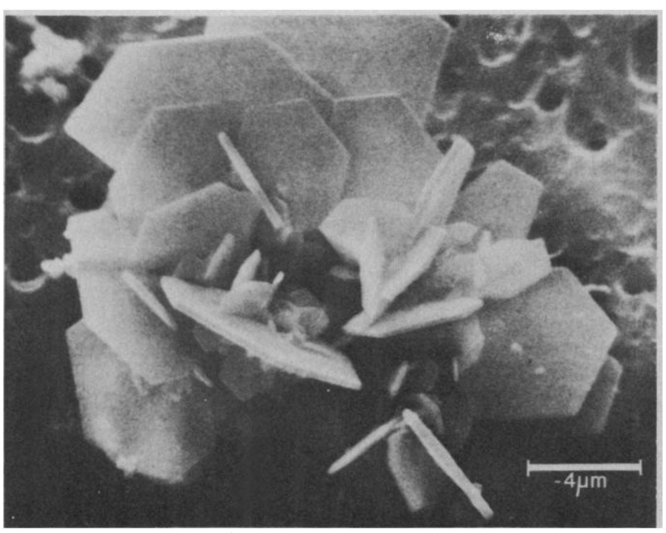

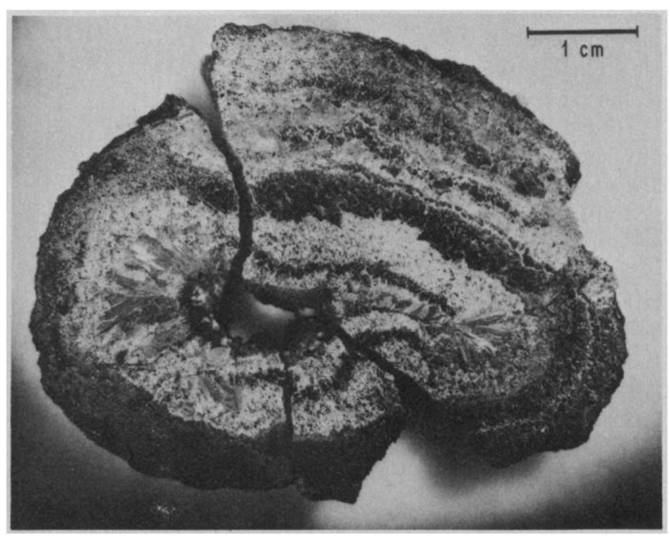

Fig. 6 (left). Scanning electron micrograph of filtered particulate pyrrhotite from hot (380° ± 30°C) waters from the black smoker shown in Fig. 4A and on the cover. Fig. 7 (right). Cross section of a small, typical chimney spire similar to those of Fig. 4A. Note concentric zonations of sphalerite, pyrite, and chalcopyrite. This zonation indicates changes in chemical and physical properties of the vents. Most zones are continuous, but the central zone of sphalerite cuts radially outward across the other zones. Both single-phase zones and zones created by intergrowth of several minerals occur in this sample.

walls of honeycomb samples are assemblages of barite and amorphous silica. Analyses to date have not fully elucidated the relationship between biogenic and inorganic mineral precipitation in the mounds.

Chimney spire samples all show radial changes in composition. Outer walls are often made of anhydrite, gypsum, and magnesium sulfate. Sulfur isotope analyses show that the anhydrite formed in equilibrium with seawater. In the innermost zones, in contact with the hot waters, are layers of coarsely crystalline chalcopyrite or pyrite. A typical small, partially closed spire (from the site shown in Fig. 4B) was studied, and a cross section of this construction revealed alternating bands of sphalerite, pyrite, and chalcopyrite (see Fig. 7). Outermost zones are enriched in amorphous silica. Cubic pyrite, the dominant phase in this sample, forms layers of different crystal sizes, which result in some of the observed banding. The three major phases are found as pure single-phase zones and as intergrowths with one other.

In addition to mound and chimney samples, near-vent sediments and basalt coatings were examined. Fine-grained black sediment scooped from the base of a black smoker contains sphalerite, pyrrhotite, pyrite, and traces of chalcopyrite, wurtzite, and sulfur. The chief phases match particulates suspended in the waters from the black smoker and represent fallout from exiting hot waters. Orange oxidized sediments collected near a dead mound exhibit a similar mineralogy. Mound fragments in these samples have higher pyrrhotite and lower pyrite concentrations than the associated sediments, indicating a rapid breakdown of unstable FeS_{1-x} to Fe-oxyhydroxide during physical disaggregation of mound materials. Rapid conversion of pyrrhotite to pyrite may explain the absence of pyrrhotite in most mound samples, or pyrrhotite may precipitate at higher temperatures within the basalt underneath the mounds. Manganese, which is largely absent from the hydrothermal mounds, precipitates hydrogenously, rather than hydrothermally, on basalt surfaces within a few meters of sulfide structures. Amorphous manganese oxyhydroxides create a dark-colored matting observed on glassy basalts around vents.

Sulfur isotope and petrographic evidence indicates that the concentric banding in active vent spires represents mineralization events that reflect changes in chemical and physical properties of the waters from which the spires precipitate. Fluctuations in temperature, pH, sulfur fugacity, and other physical and chemical parameters must occur as metal-laden solutions reach the basalt-seawater interface and traverse the lengths of the porous sulfide chimneys. These fluctuations, as well as temporal changes in the concentrations of dissolved species in the hydrothermal fluids, probably cause the observed concentric banding and may also produce vertical mineral zoning in chimneys (this possibility has not yet been investigated in detail). Considerable vent-to-vent variation in temperature was observed over relatively short distances, and seawater is undoubtedly drawn under the influence of a pressure gradient through the porous materials of mounds and chimneys to mix with rising low-density hydrothermal fluids. This inward flow of seawater allows organisms to live and grow on some chimneys and accounts for the precipitation of anhydrite in outer chimney zones.

The hydrothermal constructions sampled during the RISE program are mechanically fragile and chemically unstable in the sea floor, and they are therefore presumably ephemeral features. The iron-rich layers commonly overlying basaltic basement in Deep Sea Drilling Project (DSDP) holes (*33, 34*) may contain a component of reworked degradation products from similar vent structures. Sulfides deposited in hydrothermal conduits within the basalt layer may become sealed off from further interaction with seawater and be less susceptible to oxidation; such deposits could be the precursors of ophiolite sulfides.

Petrology of Basalts

The data presented here are based on microprobe and x-ray fluorescence analyses of glass samples collected from *Alvin* in zone 1 and along the gravity profile track of Fig. 2 and samples collected by transponder-navigated dredge hauls in zones 1, 2, and 3. This set of samples constitutes a geochemical profile across the axial region for a distance of about 3 km on each side of the axis of spreading. We wished to look for spatial and temporal variations in magma chemistry and microphenocrysts as well as any variation in magma chemistry that might be related to the morphology of the units sampled.

The glasses are fresh tan sideromelane (basalt glass) with only minor amounts of microphenocrysts of calcium plagioclase, magnesium olivine, and, in a few samples, clinopyroxene. We assume that the glass analyses represent original liquid compositions because of the apparent freshness of the samples and the small size and scarcity of the microphenocrysts. The data suggest that all of the samples experienced minor amounts of crystal fractionation (5 to 20 percent) before their eruption.

Data for the glass samples (vitrophyres) from pillow rinds, sheet flow plates, and pillow buds, as well as microphenocrysts, are summarized in Table 2. Element abundances and ratios are in Figs. 8 and 9. Samples from within about 500 m of the presumed axis of active spreading are all bright fresh glass with little or no Fe-Mn coating. Samples from greater distances have Fe-Mn coatings ranging from thin films to thicknesses of about 0.5 mm. Those with the thicker coatings (for example, > 0.1 mm) typically also have a palagonite rind of about the same thickness as the Fe-Mn crust. The palagonite and Fe-Mn crusts were removed from the glass samples that were analyzed by x-ray fluorescence. Plagioclase is the most common microphenocryst (3 to 10 percent); olivine forms 1 to 5 percent. Clinopyroxene is rare. The plagioclase forms small euhedral unzoned crystals. There is a range in plagioclase composition in individual samples which suggests that some grains are xenocrysts. The olivine is commonly irregular and skeletal in form, apparently the result of crystallization during rapid cooling. On the basis of FeO/MgO ratios of coexisting glass and olivine, the olivine appears to be in equilibrium with the enclosing glass.

Vesicles are rare, but in a few samples there are microvesicles (< 0.5 mm) which may amount to a few tenths of a percent by volume. The vesicles are decorated with sulfides, pyroxene (?), and phyllosilicates.

The samples are olivine tholeiites; all of them plot close to the presumed cotectic in the olivine-plagioclase-pyroxene diagram (Fig. 8). Abundances of K, Ti, P, Ba, Rb, Sr, Ni, and Zr are all typical of ocean ridge tholeiites (*35–37*). The samples are similar to glass samples from the FAMOUS area on the Mid-Atlantic Ridge (Fig. 9) (*37, 38*) and to other East Pacific Rise samples such as those from the CYAMEX area (*39*). The RISE samples have slightly higher values of TiO_2 and FeO*/MgO (FeO* is total iron oxides) and a smaller range of these values than many of the glasses collected on the Mid-Atlantic Ridge (Fig. 9). The limited composition range for the RISE samples collected on the 6-km-long transect suggests that the samples are derived from a common parent magma by fractional crystallization of olivine

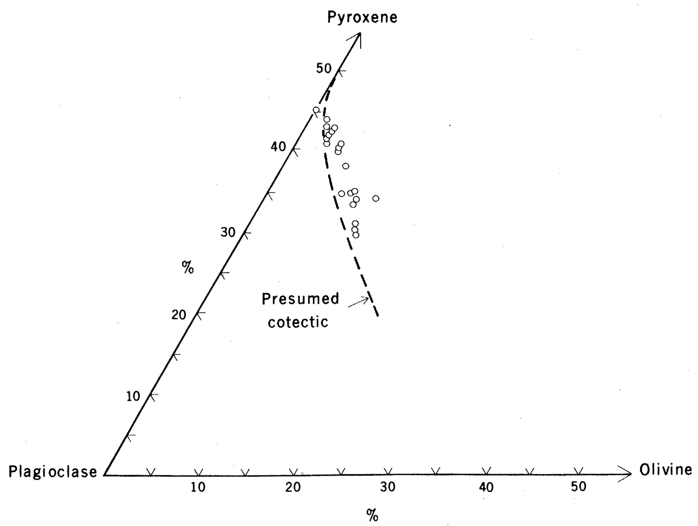

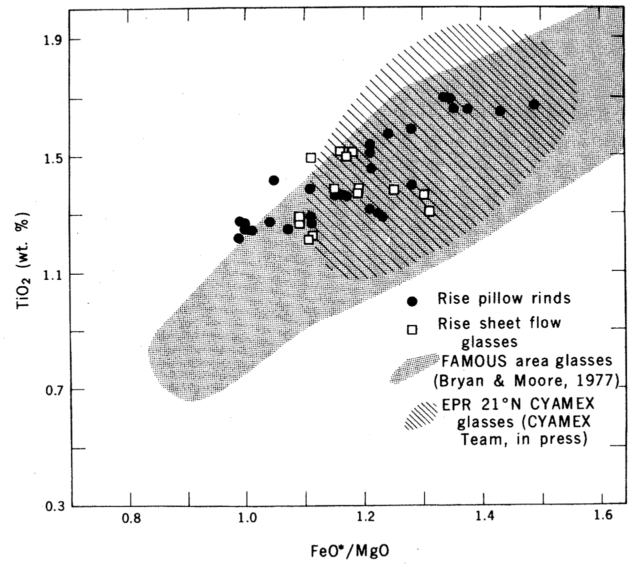

Fig. 8 (left). Electron probe analyses of RISE area glasses plotted in the pyroxene-plagioclase-olivine system. Fig. 9 (right). Plot of TiO_2 against FeO*/MgO, showing the range in fractionation for RISE samples and their relationships to basalt glasses from an adjacent area of the East Pacific Rise (CYAMEX) and those from the slower spreading Mid-Atlantic Ridge near 37°N (FAMOUS).

and plagioclase at low pressure (< 2.3 kilobars). This implies a relatively shallow (< 5 to 10 km) magma chamber. The extent of the fractionation effects on composition is shown by the range from olivine tholeiite with 11 percent normative olivine, FeO*/MgO = 1.0, 1.25 percent TiO_2, and 84 parts per million (ppm) Zr to a rock with 3 percent normative olivine, FeO*/MgO = 1.4, 1.68 percent TiO_2, 108 ppm Zr, and 128 ppm Ni. This variation may be explained by about 20 to 25 percent fractional crystallization of a mixture of plagioclase, olivine, and pyroxene (50:40:10). The postulated fractionation model was tested for major elements by mixing models (*40*) and for trace elements by Rayleigh fractionation law calculations. The simple fractionation model adequately explains the compositional range observed and is consistent with the observed phenocrysts and microphenocrysts. All the samples have Ti/Zr ≃ 90, which again implies that they were derived from a common magma type and had a common mantle source.

Eruption temperatures of the magmas were calculated by using the electron probe analyses of the glasses and the equations of Roeder and Emslie (*41*). The range of temperatures calculated by this method suggests that the least fractionated magmas [$Mg/(Mg + Fe^{2+})$ = 0.67, FeO*/MgO = 1.0, 1.25 percent TiO_2, and 158 ppm Ni] erupted at about 1220°C. The more fractionated samples [$Mg/(Mg + Fe^{2+})$ = 0.59, FeO*/MgO = 1.4, 1.68 percent TiO_2, and 128 ppm Ni] erupted at 1170°C. These temperature estimates are quite close to those reported for the CYAMEX samples (*39*). Magmaphile element abundances and the compositions of olivine and plagioclase microphenocrysts show a good correlation between calculated temperature and degree of fractionation.

We assume that since all the samples used were from the sea-floor surface, they represent the youngest eruptive material at any sample site. If a continually fractionating magma chamber has been sampled periodically and extrusion sites are concentrated at the axial zone, we should see a strong correlation between age (distance from the ridge axis and thickness of Fe-Mn-palagonite crusts) and degree of fractionation of the samples. A plot of temperature and composition against distance from the axial zone shows that although there is a broad tendency for the highest temperatures and least fractionation to occur in the central zone, there is so much scatter along the entire 6-km profile that no simple relation between composition and distance can be inferred. Off-axis samples occasionally show chemical and physical properties overlapping those of the axial zone extrusions. For example, the axial region has both young, fresh samples that erupted at a high temperature and are unfractionated [1220°C, Mg† = 0.67, where Mg† = $Mg/(Mg+Fe^{2+})$] and samples that erupted at a lower temperature and are moderately fractionated (1200°C, Mg† = 0.62). Flank samples generally are more fractionated (1170°C, Mg† = 0.59) but some overlap ridge material (1205°C, Mg† = 0.64).

It thus appears that there were fluctuations in temperature and composition with time or that the locus of extrusion varied, or both. This is in contrast with the smoother variation of properties reported for the FAMOUS area (*37*) and implies substantial differences in thermal structure and mechanisms of magma emplacement between the areas, with the RISE site representing the more complex situation.

Seismic Experiment

The seismic structure of the top several hundred meters of the oceanic crust is very poorly known because of resolution problems associated with surface sources and receivers, or even receivers on the sea floor. Rarely is a zero intercept time realized for ground-wave arrivals within a 5-km radius of the sensor. A second classical problem arises when available explosion seismology data are compared to laboratory measurements on drilled, dredged, or cored samples. In general, the in situ or seismic measurements of near-surface velocity are substantially lower than sample velocities (*42-46*). Fox *et al.* (*47*) and Spudich and Orcutt (*48*) hypothesize that the rapid increase in velocity with depth in the uppermost crust (< 600 m) is due to the effects of decreasing porosity with increasing differential pressure (lithostatic pressure minus pore fluid pressure) and depth. Certainly, laboratory samples, which are at most centimeters in dimension, lack major mechanical components such as faults and may also have been severely disrupted during recovery.

As part of the RISE program, *Alvin* and the digital ocean bottom seismographs (OBS's) of the Scripps Institution of Oceanography were used to address these two problems. Two short refraction lines, one parallel and one perpendicular to the rise crest, were "shot" to an OBS array shown schematically in Fig. 2. The seismic source was the *Alvin* rock hammer, which produced energy on the order of 1.8×10^8 ergs. The OBS's, which record digitally, were activated before each series of hammer blows by acoustic command signals initiated from *Alvin*. Accurate placement of the OBS's relative to the rise crest and surrounding topography was accomplished by lowering the instruments to within 100 to 200 m of the bottom on a trawl wire, navigating them to the chosen site by use of the acoustic transponder net, and releasing them by acoustic command. Rock samples at most stations were collected and returned to the surface for subsequent measurements of physical properties.

Two records collected at one of the stations on the 1-km legs are shown in Fig. 10. The seismograms are quite repeatable and picking the time of the first arrival is straightforward. To achieve the millisecond accuracy necessary at these short ranges, the OBS's were visited at the beginning and end of each seismic experiment dive and a series of hammer blows at ranges of 2 to 6 m were delivered. These provided a relative timing calibration between *Alvin* and the OBS's for clock corrections. The time of the hammer blows was determined on board *Alvin* by triggering a timer with 0.1 millisecond resolution with an external hydrophone near the hammer tip.

The OBS array and the site of the first hammer station (Fig. 2) were in reasonably competent pillow basalt terrane consisting of chiefly bulbous and elongate pillows. Sediment cover was extremely sparse (10 to 20 percent of the area). The pillows were fresh, as evidenced by numerous buds and ornaments, but were not characterized by the vitreous luster of the youngest basalt pillows. The OBS array and station 1 were within 500 to 600 m of the line of active hydrothermal vents (Fig. 2) and well within zone 1.

Although complete analyses are not yet available, we applied simple traveltime analysis to the station 1 arrivals (Fig. 10) to make a preliminary determination of the velocity at the surface of the crust parallel to the strike of the spreading center. While no major fissures or faults were traversed in this line, numerous hairline cracks and fissures crossed the pillows. We obtained a velocity of 3.3 km/sec, in good agreement with the mean layer 2A velocity of 3.4 km/sec (*49*) reported for crust near the East Pacific Rise and lower than the 3.8 km/sec reported by Henry *et al.* (*50*) for a crustal age slightly greater than 1 million years. Detailed inferences related to the degree of cracking and porosity necessary to produce the observations will have to await future measurements of physical properties and completion of the seismic analyses at greater ranges.

Gravity Program

Twenty-three on-bottom gravity observations were attempted, of which 20 were successful. The stations comprise a cross-strike profile about 7 km long (Fig. 2). The observations were made (i) to search for any negative gravity anomaly

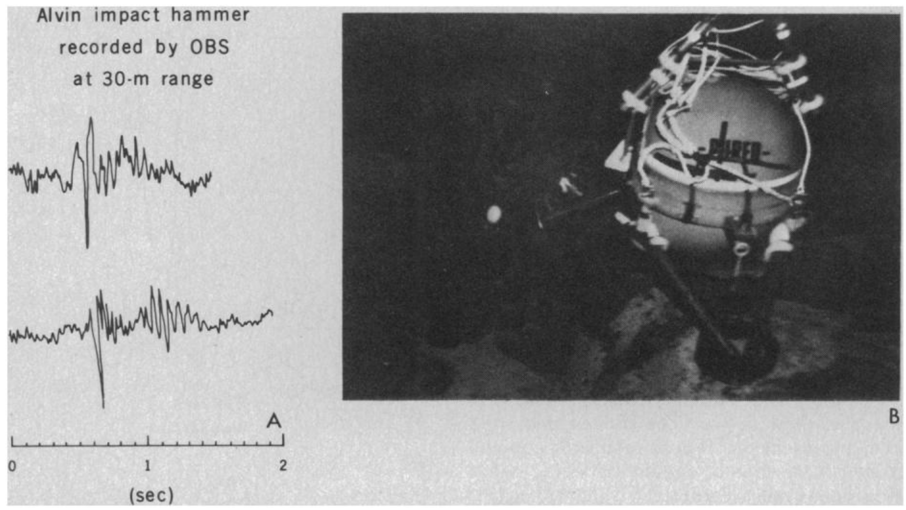

Fig. 10. (A) Two impact hammer seismograms recorded by an OBS at a range of 30 m. (B) One element of the OBS array on the sea floor at 2610 m. A near-surface in situ crustal velocity of 3.3 km/sec was determined from this station.

Table 2. Average results of analyses of basalt samples. Major elements were determined by microprobe analysis of polished glass fragments from pillow rinds, buds, and sheet flows. Percent Fe_2O_3 was calculated from total iron oxides by assuming that $Fe^{3+}/Fe^{2+} = 0.14$. Trace elements were determined by x-ray fluorescence analysis of powdered glass pressed into disks with a cellulose binder. Analytical procedures and sample preparation procedures are available from the authors.

Sample	Least fractionated glasses (N = 9)	Moderately fractionated glasses (N = 8)	Most fractionated glasses (N = 3)
	Major oxides (percent by weight)		
SiO_2	49.9	50.2	49.6
TiO_2	1.3	1.4	1.6
Al_2O_3	15.6	14.9	15.2
Fe_2O_3	1.1	1.3	1.3
FeO	7.8	8.2	8.6
MnO	0.2	0.2	0.2
MgO	8.4	7.8	7.5
CaO	11.8	11.6	11.5
Na_2O	2.7	2.8	2.9
K_2O	0.06	0.10	0.11
P_2O_5	0.1	0.1	0.2
SO_3	0.1	0.1	0.1
Cr_2O_5	0.1	0.1	0.1
Total	99.2	98.8	98.9
	Ratios		
FeO*/MgO	0.99-1.13	1.15-1.26	1.17-1.42
$Mg/(Mg + Fe^{2+})$	0.673-0.644	0.638-0.618	0.605-0.588
	Minerals (percent by weight)		
Forsterite†	87.8-85.8	86.1-84.4	85.6-84.4
Anorthite‡	85.5-69.6	83.9-68.9	79.5-67.7
	Trace elements (ppm)		
Ni	144	118	140
Zr	85	100	104
Sr	124	123	125
Ba	20	29	23
Rb	1.6	1.1	1.1

*Total iron oxides. †Microprobe analyses of olivine microphenocrysts, forsterite content. ‡Microprobe analyses of plagioclase microphenocrysts, anorthite content.

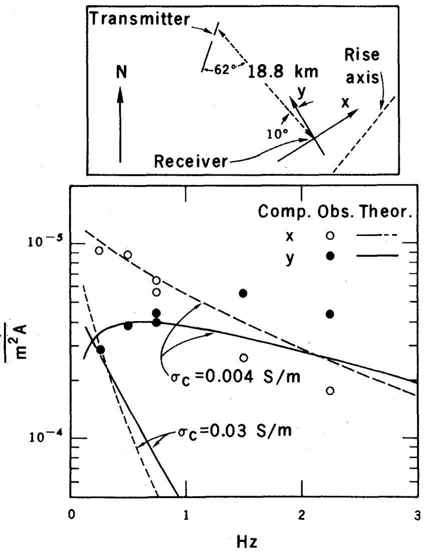

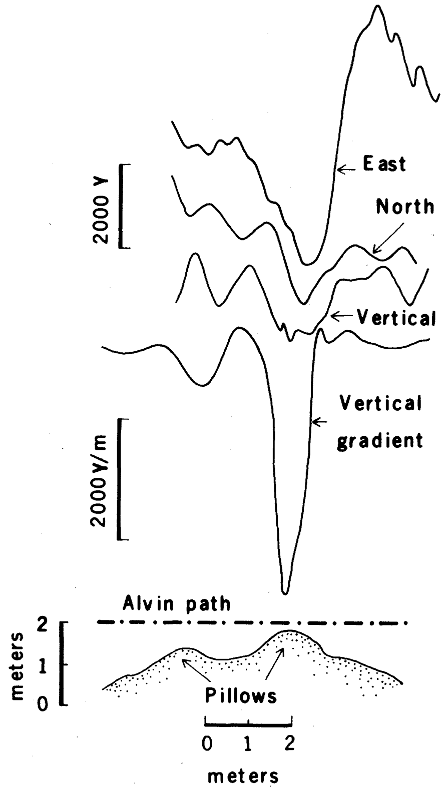

Fig. 11 (left). Ratio of received signal amplitudes (nanovolts per meter) to source dipole amplitude (ampere-meters) as a function of frequency (hertz). The open and closed circles were obtained from a preliminary analysis of the x and y components, as defined in the plan view above. The broken and solid lines represent theoretical values for a model in which the crustal conductivity, σ_c, is homogeneous and isotropic. Fig. 12 (right). *Alvin* magnetometer crossing of two negatively magnetized pillow basalts. Top three curves are the components of the field as noted; bottom curve is the vertical gradient. More than 250 clear measurements were made on either side of the polarity boundary, and all measurements showed the "correct" polarity. The boundary is very narrow, implying a narrow zone of crustal formation.

due to a shallow magma chamber or to localized pervasive fracturing of the upper ocean crust associated with hydrothermal vents and (ii) to obtain an estimate of the density of the upper crust.

The primary instrument used was a LaCoste & Romberg geodetic land meter, modified after use on the Mid-Atlantic Ridge last year (*51*), with variable damping and capacitance readout. All measurements were made with the submersible resting solidly on the sea floor. Replicate measurements were made at each station and the resulting observed precision was about 0.05 milligal ($5 \times 10^{-8}g$, where g is the gravitational acceleration).

Position control was from the transponder navigation net used for the RISE project, which is precise to about 10 or 15 m. This gives a negligible error in the latitude correction. Depth of *Alvin* (meter depth) was taken from an up-looking echo sounder transducer, which is accurate to a few meters in any region but precise to about 1 m. This could affect the precision of the gravity measurements by $\pm$ 0.2 to 0.3 mgal. Instrument drift was negligible and was not corrected for, nor was a correction attempted for earth tides. Gravity measurements were corrected to a sea-floor datum at 2556 m (uncorrected depth of the shallowest station) with the aim of enhancing local residual anomalies. For sea-floor gravity stations three corrections are needed to find the simple Bouguer anomaly relative to the sea-floor datum (*52*):

1) $+ 0.3086h$ for the decrease in g in bringing the meter up to the datum (h is datum depth minus station depth and is negative).

2) $+ 0.04319z$ for the subtractive effect of the water layer above the meter for a density of 1.03 grams per cubic centimeter (z is the water depth).

3) $-0.04193\ \sigma h$ to replace the crust between the station and the datum (σ is the Bouguer density).

The simple Bouguer anomaly needs to be corrected for the subtractive effects of the sea-floor terrane in regions surrounding each station (*53*). At this writing, the bathymetric data have not been compiled in sufficient detail to calculate these corrections fully.

A profile plot of the simple Bouguer anomaly shows it has a range of about 2 mgal (Fig. 3). However, 10 or 12 stations define a gravity low of up to 1.5 mgal with a half-width (*53*) of approximately 1.0 km. This negative anomaly is centered about the central volcanic ridge and occupies zones 1 and 2 (Fig. 2). Another gravity low appears near -2.4 km (Fig. 3), but this will be largely removed with topographic corrections.

The size and width of the central negative anomaly can be quickly analyzed in terms of a two-dimensional horizontal cylinder source. The total mass deficiency is 9×10^7 kilograms per meter of ridge. The cylinder center is at 1.0 km below the datum. If the cylinder's top edge reaches up to the datum, a minimum density contrast of 0.03 g/cm^3 is indicated. If the maximum density contrast is 0.21 g/cm^3 (rock-melt contrast), then the cylinder's top edge is 0.63 km below the datum. The density contrast in this ideal case could be due to a shallow magma chamber or crustal fracturing, or both. Further work on the *Alvin* crustal seismic travel-time data in this region may give an independent crustal density estimate to aid in resolving this question.

Crustal density was estimated by studying the correlation between observed gravity and bathymetry. The increase in observed gravity, Δg, for a station h m below the datum is $h(0.04193\ \Delta\sigma - 0.2222)$, where h is negative. A graph of Δg against h has a slope of 0.155 mgal/m. The density contrast is then 1.60, giving a rock density of 2.63 g/cm^3 between the shallowest and deepest stations.

Electromagnetic Sounding

An electromagnetic sounding technique was used during RISE to study the structure of electrical conductivity in the basement rocks near the spreading center of the East Pacific Rise. The study will provide information on the presence of conducting fluids within the upper crustal rocks.

The method of sounding involved two elements. A transmitter and a horizontal electrical dipole antenna 800 m long were dragged behind R.V. *Melville*. The antenna injected electromagnetic signals into the ocean and underlying crust at frequencies of 0.25 to 2.25 hertz. Because the signals were at relatively high frequencies, the signal in the ocean was rapidly absorbed, so that long-range signals could only have propagated within the crust. The second element consisted of three receivers that had been dropped to the sea floor from the ship before the transmissions were started. To our knowledge, no similar measurements have been attempted before, nor have any other techniques been able to provide estimates of the conductivity of the shallower crust under the oceans.

The most distant receiver was 18.8 km

away from the transmitter antenna. At this receiver the signal was clearly above noise at all the frequencies transmitted. Figure 11 shows preliminary results of the analysis of data from this receiver. The observed amplitude of the two horizontal components of the electric field normalized by the dipole strength of the transmitter antenna is shown as a function of frequency. The observed data are compared in Fig. 11 with theoretical curves derived from a simple model in which a horizontal electric dipole antenna is mounted at the plane interface between two uniform conductors representing the ocean (conductivity, 3.2 siemens per meter) and the crust (conductivity, σ_c). The comparison shows that the effective conductivity of the crust approximates 0.004 S/m. The electromagnetic skin depth of a uniform material of conductivity 0.004 S/m is 8 km for a frequency of 1 Hz. We believe this is about the effective depth of our sounding.

Previously, the conductivity of the igneous part of the oceanic crust was estimated from dredged and drilled samples (*44*) and by logging of holes drilled into basement rocks as part of the Deep Sea Drilling Project (*54*). The drilling showed that the upper part of the oceanic crust consists of basalt in many forms: pillows, massive but cracked flows, and highly fragmented pieces. The only successful deep drillings into solid rock have been in the older parts of the crust, where alteration products have plugged many fractures and vesicles. Nevertheless, the logs of electrical conductivity indicate that seawater is the dominant carrier of electricity. The results from drilling logs are widely scattered but give a geometric mean of 0.03 S/m.

The fact that our observations show an effective conductivity lower than 0.03 S/m at high frequencies may indicate that cracks and fractures are less prevalent and therefore the ability of seawater to provide conductive paths is reduced in parts of the crust below those so far drilled. The difference between the theoretically modeled and observed fields at 1.5 and 2.25 Hz is suggestive of anisotropic conductance in the upper crust, where water-filled cracks parallel to the spreading axis are expected to warp the electric field.

Magnetic Reversal Experiment

One can glean information about the earth's interior by examining the effects of naturally occurring boundaries, edges, or discontinuities on the magnetic and gravity fields. Therefore we studied the magnetic field over the Brunhes-Matuyama reversal boundary, the most recent major reversal recorded in the oceanic crust. Our goals were to determine in detail how sharp and linear the polarity transition is, and to use this information (i) to infer the width of the zone of crustal formation at the spreading center and (ii) to determine how important deep (layer 3) magnetic sources are in generating marine magnetic anomalies.

The reversal that we studied occurs 20 km west of the main RISE dive site in crust 0.7 million years old (Fig. 1). Surface ship surveys show the reversal here to be clear and linear but not unusually so (*55*). In 1977 Macdonald *et al.* (*14*) conducted a near-bottom magnetic survey over a 4 by 6 km area straddling the reversal boundary. Magnetic measurements were made on a level plane approximately 200 m above the bathymetry, using the deep-tow vehicle of the Marine Physical Laboratory (Scripps Institution of Oceanography) with precise transponder navigation. Three-dimensional modeling of the field by a Fourier inversion technique (*56*) shows that the polarity transition boundary is extremely straight and sharp and is very close to two-dimensional even on a scale of hundreds of meters. The polarity transition width is narrow, only 1000 to 1400 m throughout the study area, which suggests a zone of crustal emplacement only 600 to 1000 m wide at the spreading center (*14*).

With these results in hand, we returned to the same area with *Alvin* as part of RISE to conduct even finer scale magnetic measurements aimed at the volcanic extrusive component of the reversal boundary. A fluxgate magnetic gradiometer and three-component magnetometer were mounted in *Alvin*'s sample basket and used to make rapid, in situ determinations of crustal magnetic polarity (*57*). Typical magnetic targets were individual basalt pillows, wrinkled sheet flow ridges, and the sharp edges of fault scarps. During five geologic traverses in the reversal area, more than 250 clear in situ polarity determinations were made across the reversal boundary (Fig. 12).

In comparing the *Alvin* polarity measurements with the deep-tow inversion solution, we had several surprises. Even on long traverses (total of 4 km) to either side of the polarity boundary, every magnetic target had the correct polarity (positive or negative)—that is, a polarity that agreed with the magnetic stripes. This is not too surprising for the young side of the reversal boundary, since the newer polarity material should overlie the older. However, it is surprising that there were no outliers of newer polarity material or volcanoes on the older side of the boundary.

The reversal transition zone is very narrow. On one dive the boundary was traversed several times along a linear zone only tens of meters wide. Along strike, the reversal transition zone was actually a geologic contact; a flow (+) butted up against an axially dipping fault scarp (−), and a pillow flow front (+) facing west forming a narrow valley with a pillow flow front (−) facing east. In other places where sediment cover obscured any possible contacts, the transition from positive to negative polarity could be defined by our measurements to a zone less than 150 m wide.

The reversal boundary based on *Alvin* in situ measurements is displaced approximately 500 m away from (west of) the spreading center relative to the boundary in the deep-tow inversion solution. This offset is precisely known since the *Alvin* navigation net was linked with long-life transponders used in the deep-tow work.

When combined with the deep-tow inversion solution, the *Alvin* measurements suggest that the zone of formation of magnetic crust is very narrow. After allowing for the effects of crustal dilatation by faulting and the finite period required for the earth's field to reverse, the resultant zone of crustal emplacement is only 500 to 1000 m wide. This is in excellent agreement with geologic determinations from *Alvin* and *Cyana* for the width of zone 1, which varies from 400 to 1200 m at the present spreading axis. Thus the zone of crustal formation today and about 0.7 million years ago has been very sharply defined in space, generally less than 1 km in width.

The 500-m westward displacement of the *Alvin* determination of the reversal boundary relative to the potential field location represents spillover of basalt flows away from axial vents over older, negative-polarity crust. The width of this overlap when combined with the potential field data provides valuable information that may constrain the role of deeper sources in generating marine magnetic anomalies.

The focus of current work is to combine the *Alvin* polarity determinations with both surface-tow and deep-tow magnetic inversion solutions to sort out the extrusive and intrusive contributions to the finite width of the field reversal recorded in the crust. From this we hope to place bounds on the width of volcanism, the width of dike intrusion, and the importance of layer 3 sources such as gabbro in generating marine magnetic anomalies.

Summary of Geophysical Experiments

All four geophysical experiments were prototypes, and it is difficult this soon after the cruise to have complete results or to merge them with the geological and hydrothermal observations. However, the combined research efforts are taking several interesting directions. Combination of the seismic and gravity results should resolve the question of whether the axial gravity anomaly is caused by a shallow magma chamber or surficial fissuring (we suspect the former). These results in turn will be combined with inferences about the magma chamber from the petrologic studies. While the gravity and seismic studies may indicate the presence and depth of a magma chamber near the axis, the electrical studies may indicate its width by sensing high conductivity at depth off-axis. The seismic and electrical studies should place bounds on the depth of fissuring of the crust and, combined with the hydrothermal observations, be used to determine the depth of hydrothermal circulation along the axis. The magnetic studies in the reversal area already suggest a narrow zone of crustal formation that has been stable for some time and agree well with the geological observations. The magnetic studies should also indicate how important deeper layer 3 sources and cumulate settling portions of the magma chamber are as sources of lineated magnetic anomalies.

Conclusions

The axis of the East Pacific Rise is marked by a zone of recent volcanism approximately 1000 m wide. Near the center of the volcanic zone, there is a very narrow band of active hydrothermal vents—at least 25 vents along a strip 7 km long and only 200 to 300 m wide. In the northeast, vents are characterized by water temperatures of 5° to 20°C, flow rates of centimeters per second, clear vent waters, and exotic biological communities similar to those at the Galápagos vents (giant tube worms, clams, galatheid crabs). These communities, independent of photosynthesis for survival, must have unusual dispersal systems that allow them to populate various areas of the world rift system as hydrothermal vents evolve and die out. To the southwest, vent waters contain more particulate matter, often dark in color (black smokers); the exit temperatures reach 380° ± 30°C; flow rates are on the order of several meters per second; and conditions appear less inviting for the biological communities near the vents, except for a new polychaete, which may live at very high temperatures. The marked along-strike variation may indicate an evolutionary cycle in the development of the vent system. Actively forming massive sulfide deposits occur within the vent chimneys at high-temperature springs, while inactive sulfide mound deposits occur slightly off-axis from the cooler vents. Mineral deposits include sphalerite, pyrite, chalcopyrite (and other Fe, Cu, and Zn sulfides), anhydrite, sulfur, barite, opal, and talc. Chimneys exhibit a distinct concentric zoning of sulfide minerals, which suggests episodicity in the physical and chemical properties of the vents. The hydrothermal waters contain the first such occurrences of pyrrhotite and other sulfide compounds as well as methane. Covariance of methane with ^3He indicates a mantle source for both. There is substantial evidence for biological influence on the mineral deposits; for example, worm-tube honeycomb structures form the foundations for many sulfide mounds.

Basalt samples from the spreading center have a narrow range of chemical composition and are extremely primitive. They probably formed by fractional crystallization from a shallow magma chamber, possibly from a single parent magma.

Alvin has been used for the first time as a geophysical tool. The on-bottom gravity and seismic measurements have yielded the first in situ determinations of shallow crustal seismic velocity and density. Further analysis of the gravity, seismic, and electrical data should place bounds on the depth of hydrothermal activity and crustal fissuring, and determine the extent of the axial magma chamber. Magnetic measurements at the reversal boundary indicate a narrow (500 to 1000 m) zone of crustal formation, and may place bounds on the role of deep crustal sources in generating marine magnetic anomalies.

References and Notes

1. K. C. Macdonald and F. N. Spiess, *Scripps Inst. Oceanogr. Ref. 76-18* (1976).
2. T. Atwater and J. D. Mudie, *J. Geophys. Res.* **78**, 8665 (1973).
3. R. L. Larson and F. N. Spiess, *Science* **163**, 68 (1969).
4. K. C. Macdonald and B. P. Luyendyk, *Geol. Soc. Am. Bull.* **88**, 621 (1977).
5. K. D. Klitgord and J. D. Mudie, *Geophys. J. R. Astron. Soc.* **38**, 563 (1974).
6. FAMOUS was the French-American Mid-Ocean Undersea Study carried out in 1971 to 1974 on the Mid-Atlantic Ridge rift valley and adjacent fracture zones near 36°50′N.
7. J. R. Heirtzler and Tj. H. van Andel, *Geol. Soc. Am. Bull.* **88**, 481 (1977).
8. ARCYANA, *Science* **190**, 108 (1975).
9. R. D. Ballard, W. B. Bryan, J. R. Heirtzler, G. Keller, J. G. Moore, Tj. H. van Andel, *ibid.*, p. 103.
10. J. B. Corliss *et al.*, *ibid.* **203**, 1073 (1979).
11. F. N. Spiess, C. D. Lowenstein, D. E. Boegeman, J. D. Mudie, in *Oceans '76* (Institute of Electrical and Electronics Engineers and Marine Technology Society, Washington, D.C., 1976).
12. R. L. Larson, *Geol. Soc. Am. Bull.* **82**, 823 (1971).
13. W. R. Normark, *Geology* **4**, 681 (1976).
14. K. C. Macdonald, S. P. Miller, S. P. Huestis, F. N. Spiess, *J. Geophys. Res.*, in press.
15. W. R. Normark, T. R. Alpha, G. R. Hess, G. S. Lichtman, C. E. Gutmacher, *U.S. Geol. Surv. Open-File Rep. 78-350* (1978); W. R. Normark, *Mar. Geod.* **3**, 29 (1979).
16. CYAMEX Science Team, *Mar. Geophys. Res.*, in press.
17. _____, *Nature (London)* **277**, 523 (1979).
18. The two submersible operations, CYAMEX and RISE, plus a third scheduled for the Tamayo Fracture Zone in October 1979 have been linked together as a Mexican-French-U.S. program designated RITA (Rivera-Tamayo). Although the first was primarily supported by France and the second by the United States, there has been full participation in planning, sea operations, and reporting by scientists from all three countries.
19. *Woods Hole Notes* **1**, 2 (1979).
20. R. D. Ballard, R. T. Holcomb, Tj. H. van Andel, *J. Geophys. Res.*, in press.
21. J. Francheteau, T. Juteau, C. Rangin, in preparation.
22. R. F. Weiss, P. F. Lonsdale, J. E. Lupton, A. E. Bainbridge, H. Craig, *Nature (London)* **267**, 600 (1977).
23. P. F. Lonsdale, *Earth Planet. Sci. Lett.* **36**, 92 (1977).
24. _____, *Deep-Sea Res.* **24**, 857 (1977).
25. J. B. Corliss, J. Dymond, M. Lyle, K. Crane, *Earth Planet. Sci. Lett.* **40**, 12 (1978).
26. Galápagos Biology Expedition Participants, *Oceanus* **22**, 2 (1979).
27. W. A. Newman, *Trans. San Diego Soc. Nat. Hist.*, in press.
28. H. W. Jannasch and C. O. Wirsen, *BioScience*, in press.
29. J. Lupton, G. Klinkhammer, W. Normark, R. Haymon, K. Macdonald, R. Weiss, H. Craig, in preparation.
30. J. A. Welhan and H. Craig, *Geophys. Res. Lett.*, in press.
31. W. Seyfried and J. Bischoff, *Earth Planet. Sci. Lett.* **34**, 71 (1977).
32. M. J. Mottl and H. D. Holland, *Geochim. Cosmochim. Acta* **42**, 1103 (1978).
33. C. C. von der Borsch and R. W. Rex, in *Initial Reports of the Deep Sea Drilling Project*, D. A. McManus *et al.*, Eds. (Government Printing Office, Washington, D.C., 1970), vol. 5, p. 541.
34. D. S. Cronan *et al.*, *Science* **175**, 61 (1972).
35. A. E. J. Engel, C. G. Engel, R. G. Havens, *Geol. Soc. Am. Bull.* **76**, 719 (1965).
36. W. G. Melson, T. L. Vallier, T. L. Wright, G. Byerly, J. Nelen, in *The Geophysics of the Pacific Ocean Basin and Its Margin* (American Geophysical Union, Washington, D.C., 1976), p. 351.
37. W. B. Bryan and J. G. Moore, *Geol. Soc. Am. Bull.* **88**, 556 (1977).
38. W. B. Bryan, *J. Petrol.* **20**, 293 (1979).
39. CYAMEX Science Team, in preparation.
40. T. L. Wright and P. C. Doherty, *Geol. Soc. Am. Bull.* **81**, 1995 (1970).
41. P. L. Roeder and P. F. Emslie, *Contrib. Mineral. Petrol.* **29**, 275 (1970).
42. E. Schreiber and P. J. Fox, *J. Geophys. Res.* **81**, 4071 (1976).
43. _____, *Geol. Soc. Am. Bull.* **88**, 600 (1977).
44. R. D. Hyndman and M. J. Drury, *J. Geophys. Res.* **81**, 4042 (1976).
45. N. I. Christensen and M. H. Salisbury, *Earth Planet. Sci. Lett.* **19**, 461 (1973).
46. N. Warren and B. Rosendahl, in *Initial Reports of the Deep Sea Drilling Project* (Government Printing Office, Washington, D.C., in press), vol. 54.
47. P. J. Fox, E. Schreiber, J. J. Peterson, *J. Geophys. Res.* **78**, 5155 (1973).
48. P. Spudich and J. Orcutt, *ibid.*, in press.
49. R. E. Houtz, *ibid.* **81**, 6321 (1976).
50. M. Henry, L. Dorman, J. Orcutt, *Eos* **59**, 1138 (1978).
51. B. P. Luyendyk, in preparation.
52. L. L. Nettleton, *Gravity and Magnetics in Oil Prospecting* (McGraw-Hill, New York, 1976).

53. S. Hammer, *Geophysics* 4, 184 (1939).
54. R. J. Kirkpatrick, in *Initial Reports of the Deep Sea Drilling Project*, L. Dmitriev *et al.*, Eds. (Government Printing Office, Washington, D.C., 1979), vol. 46, p. 401.
55. R. L. Larson, *Scripps Inst. Oceanogr. Ref. 70-2* (1970).
46. R. L. Parker and S. P. Huestis, *J. Geophys. Res.* 79, 1587 (1974).
57. T. M. Atwater and K. C. Macdonald, *Eos* 59, 1198 (1978).
58. We acknowledge the highly competent support provided by *Alvin*'s operators, led by pilots D. Foster, R. Hollis, and G. Ellis; the crews of R.V. *Lulu* (J. Boord, master), R.V. *Melville* (A. Arsenault, master), and R.V. *New Horizon* (A. Phinney, master); and the members of the several hardworking scientific parties. F. Grassle and J. Kerridge made substantial contributions through analyses and descriptions of biological and mineralogical samples. L. Shure aided in the collection and analysis of the magnetic data. The expedition was funded by the Seabed Assessment Program of the National Science Foundation International Decade of Ocean Exploration office under grants NSF/OCE 78-01664, 78-21082, and 79-09984. Funds for mineralogical and geochemical analyses were provided by a grant from the Academic Senate, University of California, San Diego. Support for the electrical measurements was provided by the National Science Foundation and the Office of Naval Research (Earth Physics Branch).

Sulfide Deposits from the East Pacific Rise Near 21°N

R. Hekinian, M. Fevrier, J. L. Bischoff, P. Picot, W. C. Shanks

Summary. Massive sulfide deposits were discovered from the diving saucer *Cyana* on the accreting plate boundary region of the East Pacific Rise near 21°N. The deposits form conical and tubular structures lying on a basaltic basement. Mineralogical and geochemical analyses showed two main types of intimately associated products: a polymetallic sulfide-rich material composed of pyrite and marcasite in association, zinc-rich phases, and copper-rich compounds, and an iron-rich oxide and hydroxide material (also called gossan) composed largely of goethite and limonite. Silicate phases such as opaline, silica, iron-silicon clay, and trace amounts of mica and zeolite are encountered in both types of material. Possible mechanisms for the formation of the sulfide deposits on the East Pacific Rise are discussed.

The early discoveries of hydrothermal products at accreting plate boundaries were sediments rich in iron and manganese (*1*). More recent findings of strongly fractionated iron-manganese concretions, material rich in silicon-iron clay, and hydrous iron oxides have been collected from the Galápagos spreading center (*2, 3*), from the Mid-Atlantic Ridge near 26°N (*4, 5*) and 37°N (*6*), and from the Gulf of Aden (*7*). Direct visual observations of thermal springs were made during a submersible study on the rift valley of the Galápagos spreading center (*8*).

The first discovery of a sizable submarine polymetallic sulfide deposit on a ridge system was made in the Red Sea during the international Indian Ocean expedition (1963 to 1965). In addition, many ancient massive sulfide deposits found in ophiolites are thought to have been formed on the sea floor in large oceans or marginal basins. These deposits consist primarily of pyrite, chalcopyrite, and sphalerite (*9–12*). The ophiolitic massive sulfide deposits, such as those in the Troodos complex in Cyprus (*13*), Semail in Oman (*14*), and Betts Cove and York Harbor in Newfoundland (*12, 15*), appear to represent ancient oceanic crust formed at mid-oceanic spreading ridges. A summary of the ophiolite complexes containing sizable ore deposits around the world is given by Coleman (*16*).

A recently formed massive sulfide deposit with similarities to the ophiolitic deposits was recently discovered by a manned submersible on the East Pacific Rise at 21°N during a French-American-Mexican joint project (project RITA) on rapidly spreading ridges (*17, 18*) (Fig. 1). The East Pacific Rise deposit occurs at a spreading ridge at 21°N. The rate of separation at the site, 3 centimeters a year, appears to have been constant during the last 4 million years (*18*). As indicated by deep-tow studies (*19*), the ridge crest in the area is dominated by a central zone of volcanic hills about 2 to 5 kilometers wide flanked on either side by a zone of open fissures.

More recent dives in the region by the submersible *Alvin* have discovered other massive sulfide mounds and actively discharging hydrothermal vents and solid particles with fluid temperatures of 375° ± 25°C (*20, 21*). Conical plumes discharging sulfide minerals on the sea floor were recently predicted by Solomon and Walshe (*22*) from experimental studies of deposits of the Cyrpus and Kuroko type. We present here the results of mineralogical and geochemical studies of sulfide deposits during dives of the submersible *Cyana* at 21°N (*23*).

Geologic Setting of the Sulfide Deposit

The deposits were sampled at two sites (Cy 78-08 and Cy 78-12) located on the flanks of steep-sided structural depressions about 20 to 30 meters deep and 20 to 30 meters wide, situated 700 to 800 meters west of the axis of the East Pacific Rise (Fig. 1) (*17*). The general area consists of a 1.5-km-wide band of fissured and faulted terrane associated with a horst and graben zone (*17, 24*). The massive sulfide deposits form roughly cylindrical hills ranging up to 10 m high and averaging 5 m in diameter (*23*). In an area visited during dive Cy 78-8, at least three vertical hills aligned in an approximately north-south direction (025°) were seen over a distance of about 50 m. The hills are about 3 to 4 m apart and the flanks of two different hills could be seen from the porthole of the submersible when it passed between them. The edifices are variegated with ocher, red, white, and dark gray colors and appear to be extremely porous. The first sample (8-14A) was taken on a tall hill (approximately 10 m high) and consists of a brownish-red ocher-like material. The second sample was taken about 10 m away from the first on the same hill.

The authors' affiliations are: R. Hekinian, Centre Océanologique de Bretagne, Brest Cédex 29273, France; M. Fevrier, Centre Océanologique de Bretagne and Université de Bretagne Occidentale, Brest Cédex 29200; J. L. Bischoff, U.S. Geological Survey, Menlo Park, California 94025; P. Picot, Bureau de Recherche Géologique et Minière, Orleans Cédex 45018; and W. C. Shanks, Department of Geology and Geophysics, University of Wisconsin, Madison 53706.

0036-8075/80/0328-1433$02.00/0